WARSAW UNIVERSITY OF TECHNOLOGY Index 351733
FACULTY OF CIVIL ENGINEERING
COMMITTEE FOR CIVIL AND WATER ENGINEERING
POLISH ACADEMY OF SCIENCES ISSN 1230-2945

DOI: 10.24425/ace.2024.149880

ARCHIVES OF CIVIL ENGINEERING

Vol. LXX ISSUE 2 2024

pp. 543 –560

© 2024. Xilong Zheng.

This is an open-access article distributed under the terms of the Creative Commons Attribution-NonCommercial-NoDerivatives License (CC BY-NC-ND 4.0, https://creativecommons.org/licenses/by-nc-nd/4.0/), which permits use, distribution, and reproduction in any medium, provided that the Article is properly cited, the use is non-commercial, and no modifications or adaptations are made.

Research paper

Research on construction monitoring of curvilinear continuous beam bridge jacking and horizontal moving construction

Xilong Zheng[1]

Abstract: This article investigates the issue of beam misalignment in continuous curved beam bridges. Taking the D0–D6 spans of the Gongbin Road elevated bridge as a basis, real-time monitoring of the stress and displacement of the beams is carried out during the jacking and shifting construction process. At the same time, the reaction forces of each support are monitored. The jacking force of the hydraulic jacks is controlled to ensure the stability and safety of the beam during the construction process. Finally, the jacking and shifting monitoring data is organized and compared with theoretical values. It is found that the stress values generated during the jacking phase of the bridge are below the stress control standard. No uplift phenomenon occurs at the supports, and the jacking height is controlled within a reasonable range. The construction process does not cause damage to the beams, and it is safe and reliable. During the shifting construction, the whole bridge was displaced using the jacking method, and the three working conditions were monitored throughout the process. The stress increment at the 2# and 4# sections was relatively small, and the measured stress increments for the entire bridge were all below the stress control standard. The displacement of the bridge abutment during the jacking process was minimal, with no contact with the abutment blocks, and no significant elastic deformation occurred. The jacking displacement was successfully achieved.

Keywords: continuous beam bridge, jacking construction, shifting construction, construction monitoring

[1]PhD., Harbin University, School of Civil and Architectural Engineering, No.109 Zhongxing Da Dao, Harbin, China, e-mail: sampson88@126.com, ORCID: 0000-0001-5571-667X

1. Introduction

With rapid economic development and continuous technological advancements, China's transportation industry has witnessed a new era, particularly in the field of highway bridge development, achieving remarkable achievements. Due to their large numbers and significant importance, the daily maintenance and repair work of these bridges deserves more attention [1–3]. Due to being mostly constructed in the previous century, these bridges are limited by the technology available at that time, and their design load standards and capacity cannot meet the current requirements [4]. Currently, the investment in highway bridge construction in China is mainly focused on large-scale bridges, while the funding for small and medium-span bridges is limited. For those small and medium-sized bridges that cannot meet current traffic requirements, it is almost impossible to demolish and rebuild them. Instead, it is necessary to retrofit the existing bridges to meet the current traffic demands [5, 6].

Synchronous jacking technology has been rapidly promoted and widely applied as the highway bridge and culvert industry continues to develop. The weight and height requirements for jacking are constantly increasing [7, 8]. However, there is still a certain gap between the current synchronous jacking technology for bridges and the actual engineering requirements. There are no specific regulations or guiding documents for the design and construction of bridge misalignment, and the methods to address misalignment mainly rely on previous construction experience. The study on the stress characteristics and deformation extent of the beam during jacking and translation processes is not clear, especially for complex bridge structures with large spans, long distances, and heavy loads, which lack in-depth exploration [9–12]. Moreover, during construction, there is a lack of state monitoring and effective control measures for the jacking and translation processes, which poses risks to both construction and the subsequent operation of the bridges [13–15]. This article proposes a practical construction scheme for jacking and translation, and conducts monitoring and analysis during the construction process to validate the effectiveness of simulation analysis. It provides a basis for the design and construction of jacking and translation for future bridge projects.

2. Engineering background

The Gongbin Road elevated bridge system is located in Harbin city and designed with load rating level of City Class-A. The main section of the Gongbin Road elevated bridge system consists of a total of 119 spans. This study focuses on the displacement analysis of spans D0 to D6. The upper structure of spans D0 to D6 consists of a six-span continuous cast-in-place reinforced concrete curved box beam. The span combination is $20 + 4 \times 25 + 20 = 140$ m. The box beam is a two-box six-cell structure with a height of 1.4 m. The total width of the bridge deck for spans D0 to D6 is 28 m. The bridge width layout: 0.5 m crash barrier + 12.0 m roadway + 2.0 m median strip + 12.0 m roadway + 0.5 m crash barrier. The substructure for piers D1 to D5# consists of column-type bridge piers,

while pier D6 is a prestressed concrete inverted T-shaped cap beam pile and column-type bridge pier. The abutment adopts a reinforced concrete rectangular abutment. The actual view of the elevated structure is shown in Fig. 1, while the elevation, plan, and cross-section drawings of the bridge are shown in Fig. 2 to Fig. 4.

Fig. 1. Actual view of the elevated bridge

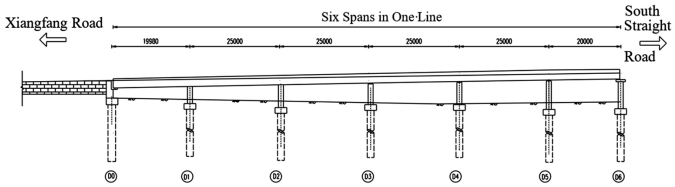

Fig. 2. Bridge elevation layout diagram

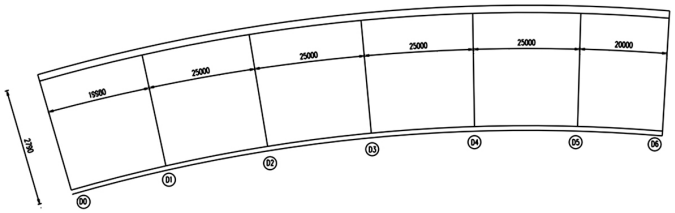

Fig. 3. Plan layout diagram

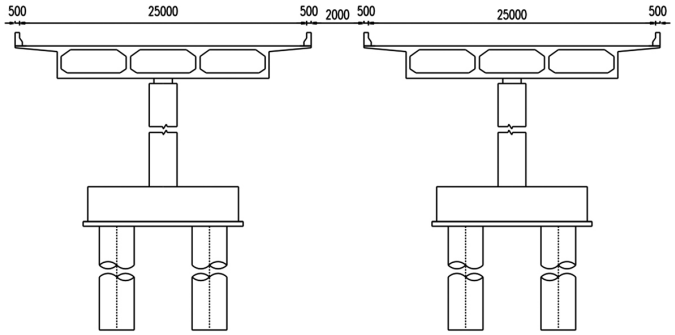

Fig. 4. Cross-section layout diagram

3. Offset distortion

During the inspection of the curved continuous beam bridge, it was found that the main girder showed significant lateral creep towards the outside of the curve. The D6# pier box girder exhibited the most significant lateral creep, with a measured transverse displacement of at least 90 mm at the abutment on the outside of the curve. Due to the lateral creep of the continuous box girder, significant structural damage has occurred to its lower bearings, bridge piers, and even adjacent ramp bridges. At the end of the 6# pier cap beam (on the outside of the curved beam), the block that serves as a barrier has fractured due to the lateral compression from the main girder, posing a risk of falling, as shown in Fig. 5.

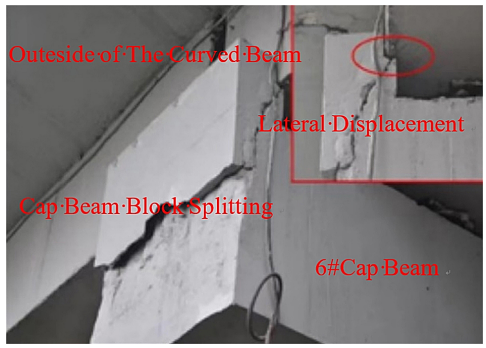

Fig. 5. Diagonal splitting of the cap beam block on the bridge pier

The lateral creep of the curved beam bridge causes the steel plates on the bearings to move together. Inspection revealed a common occurrence of lateral displacement of the upper steel plate in bidirectional movable supports. In certain cases, there is a significant 40 mm offset between the upper steel shim plate and the steel pot, as shown in Fig. 6 and Fig. 7.

Fig. 6. Lateral limiting steel bar under compression deformation

Fig. 7. Slippage of steel plate out of steel pan by 40 mm on bi-directional support

There are multiple semi-circular cracks on the outer side of the lower part of the bridge pier column, as shown in Fig. 8. The maximum width of the cracks is 0.26 mm. The schematic diagram of crack distribution is shown in Fig. 9. The analysis indicates that the presence of fixed bowl-type bearings on top of the pier is the likely cause. The tendency of the main beam to move outward is constrained by the fixed bearings. According to the principle of force interaction, the main beam exerts a radial force on the bearings in the direction of creep. This results in a transition of the pier column from an axially compressed state to an eccentrically compressed state, and even induces tensile stress on the outer side of the concrete.

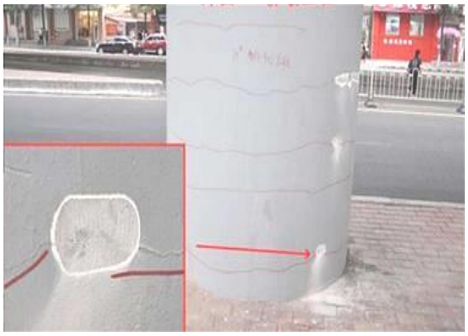

Fig. 8. Semi-circular cracking in the concrete at the base of column

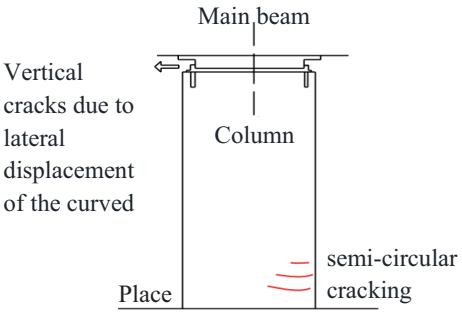

Fig. 9. Illustration of cracks in the column

4. Jack-up and translation construction process

The step-by-step jacking and translation plan for the Gongbin Road overpass is as follows: The spans from D0 to D6 do not have overhead beam pier caps, and the space around the pier cap bearings is narrow, making it impossible to place the jacks on the pier caps. Based on the actual situation, steel clamps or steel outriggers are installed on the bridge piers to vertically jack up the beam and laterally translate it. The steps are as follows:

1. Installation of steel outriggers/steel clamps.
   Transport the prefabricated steel clamps to the side of the pier, then embed the reinforcement in the pier body and establish alignment and hole layout for the pier. The hole diameter is 300 mm with a depth of 330 mm. Before drilling, a rebar detector should be used to determine the position of the main reinforcement for adjusting the hole position as required by the drawings. Install the steel clamps and tighten the side connecting bolts before embedding the reinforcement to ensure a tight fit between the steel clamps and the pier. Before embedding the reinforcement, inspect the installation of the steel clamps and check if the welding work has been completed. The on-site construction is shown in Fig. 10 and Fig. 11.

Fig. 10. Pier column drilling

Fig. 11. Reinforcement with hoop bars

Due to the large tensile force on the upper anchor bolts caused by eccentric moment, the spacing between the anchor bolt groups does not meet the code requirements. Therefore, pre-stressing is applied to the steel hoop bars to reduce the tensile force on the upper anchor bolts and ensure that the concrete will not be subjected to tension and damaged. The specific construction method is shown in Fig. 12.

Fig. 12. Prestressing of hoop bars

2. Installation of jacking equipment
   Paste leveling steel plate or set universal hinge at the jacking position under the beam. Place a 3 mm rubber sheet at the jacking location on the top of the steel hoop. Install a 650 t hydraulic jack with mechanical lock. Place a 2 mm thick rubber sheet on the top surface of the jack.
3. Pre-compress and grout the gap between the steel hoop and the pier body
   Apply 50% counter-pressure on the steel hoop to ensure proper anchoring, then grout the gap between the steel hoop/bull's leg and the pier body to seal it with grout, ensuring that it will not be damaged by force during the curing process. Apply edge sealant on the steel plate and inject adhesive grout.

4. Bridge jacking and removal of existing bearings
   Position and pad the temporary steel shims and jacks, and carry out a trial jacking of the approach bridge to inspect the performance of the jacking and sliding devices, and to verify if the steel leg or steel hoop can meet the requirements. Proceed with the formal jacking of the beam, employing a step-by-step approach, with each increment controlled within 5–10 mm, until a total lifting height of 80 mm is reached. After lifting the beam to the predetermined height, remove the existing bearings and carry out treatment on the bearing pad stones, as shown in Fig. 13 and Fig. 14.

Fig. 13. Construction drawing for jacking operation (1)

Fig. 14. Construction drawing for jacking operation (2)

5. Installation of steel slide rail and beam placement
   After removing the original pot-type bearings, install the steel slide rail and lower the beam onto the steel slide rail. The arrangement of the slide rail system from top to bottom is as follows: Oil is applied on the top surface of the steel plate to reduce the friction coefficient between the PTFE board and the stainless steel plate. The purpose of the rubber pad is to increase the friction coefficient between the PTFE board and the beam bottom, as shown in Fig. 15.

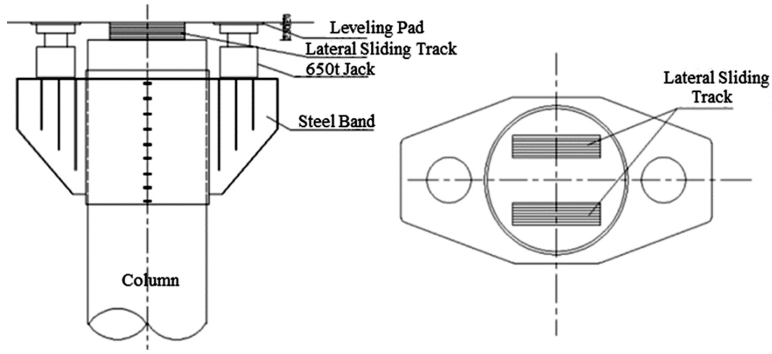

Fig. 15. Arrangement diagram of beam resting on piers on the sliding track (single-column pier)

6. Installation of horizontal alignment correction device/limitation device

(a) Installation of horizontal alignment correction device
After the beam is placed on the steel sliding track, install horizontal steel legs and horizontal jacks. The selected capacity for the horizontal jacks is 150 t, based on the criterion that the tonnage should be greater than or equal to 0.1× (dead load ×1.2+ live load ×1.4), as shown in Fig. 16.

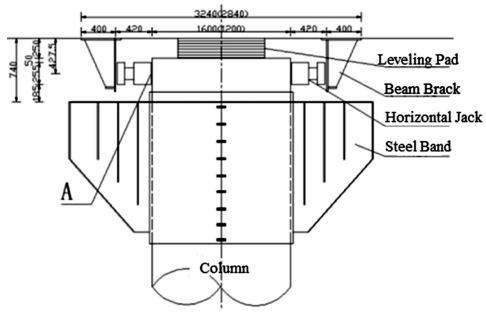

Fig. 16. Diagram of horizontal braces and horizontal jack layout

(b) In the process of horizontal alignment during construction,
The shared piers D0# and D6# can only rotate and not displace. In order to prevent accidents such as excessive displacement and beam collapse during the jacking and alignment process, limit devices are installed on the shared piers D0# and D6#. Beam braces are set on the bridge abutment, and inverted L-shaped braces are set on the bottom of the beam, thereby interlocking with each other to provide limiting effect, as shown in Fig. 17.

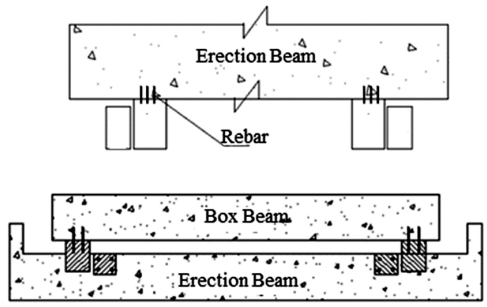

Fig. 17. Limit switch diagram

7. After the main bridge body is laterally shifted and the lateral shifting device is installed, the horizontal jacking restart construction is carried out with a jacking speed of less than 1mm/min. After the jacking restart, the horizontal jacks and horizontal steel supports will be removed, as shown in Fig. 18 and Fig. 19.

Fig. 18. Beam translation (a)

Fig. 19. Beam translation (b)

8. After the replacement of the bearings is rectified, install the vertical jacks and incrementally lift the beam by 2 mm, remove the steel sliding rails, and install new bearings.
9. After the replacement of the bearing supports is completed, perform incremental beam lowering. During the beam lowering process, all jacks shall simultaneously retract oil in synchronization, strictly controlling the synchronous lowering of each support point in the same set. The synchronized descent hydraulic system is controlled by a computer to complete this operation.

5. Construction monitoring plan

5.1. Arrangement of construction monitoring points

Bridge lifting and horizontal displacement construction monitoring mainly involve stress monitoring and displacement monitoring. The schematic diagram in Fig. 20 illustrates the cross-sectional view for stress and displacement monitoring during the lifting process. During the lifting operation, 3 stress measurement points equipped with strain gauges are installed at the bottom of each cross-sectional beam, as shown in Fig. 21. Additionally, 3 vertical displacement control points equipped with dial gauges are arranged at the bottom of each cross-sectional beam, as shown in Fig. 22. The strain monitoring measurement points and displacement monitoring measurement points are shown in Fig. 23 and Fig. 24.

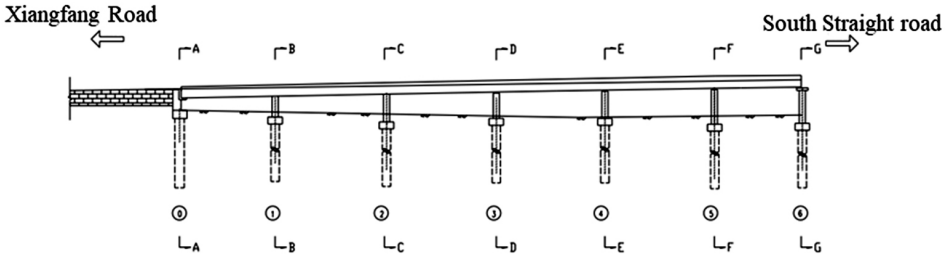

Fig. 20. Schematic diagram of lifting and horizontal displacement monitoring section

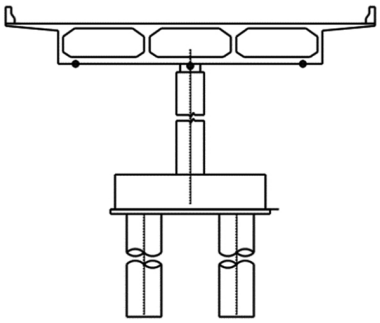

Fig. 21. Schematic diagram of lifting stress monitoring points

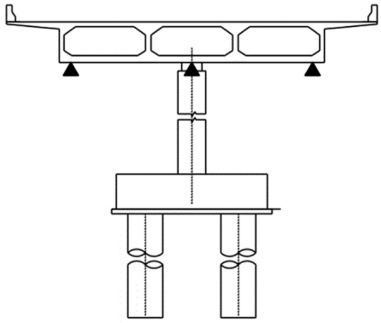

Fig. 22. Schematic diagram of lifting displacement monitoring points

Fig. 23. Strain monitoring measurement points

Fig. 24. Displacement monitoring measurement points

During translation, two control points with steel-string strain gauges are arranged at the bottom and web plate of each cross-section beam, as shown in Fig. 25. Additionally, two transverse displacement control points are arranged on both sides of the web plate of each cross-section beam, as measured using dial gauges, as shown in Fig. 26. Furthermore, the entire bridge is monitored for displacement using a total station. The monitoring frequency is to collect data once per 2 mm lift.

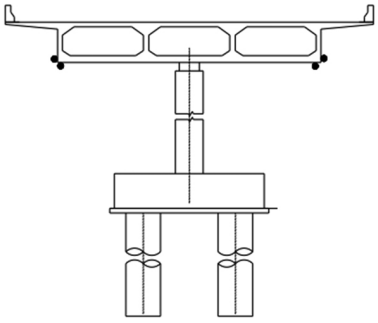

Fig. 25. Schematic diagram of lifting displacement monitoring points

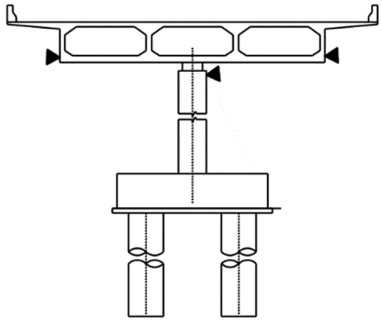

Fig. 26. Schematic diagram of jacking displacement monitoring points

During monitoring of jacking and translation construction, the readings of each measuring point should be obtained for each load level. It is advisable to place the gauge on nearby brackets to avoid any influence from pier deformation. Additionally, detailed data of each test section and key areas should be documented before construction, along with simultaneous recording of atmospheric temperature.

6. Monitoring data and analysis

6.1. Analysis of monitoring data during the jacking process

The displacement, stress, and jack thrust results when the jacking beam reaches 3.0 cm are shown in Table 1 and Fig. 27 to Fig. 29. The inside displacement of the curve is about 30 mm when the jacking beam reaches 3.0 cm. The thrust is from 2194 kN to 2912 kN. The concrete stress is from –0.04 MPa to 1.03 MPa. The outside displacement of the curve is about 30 mm when the jacking beam reaches 3.0 cm. The thrust is from 2366 kN to 3812 kN. The concrete stress is from 0.03 MPa to 1.11 MPa.

Table 1. Displacement, Stress, and Jack Thrust Values Corresponding to the synchronous jacking of the bridge by 3.0 cm

Serial number	Number of jacks	Inside of the curve			Outside of the curve		
		Elevation (mm)	Thrust (kN)	Stress (MPa)	Elevation (mm)	Thrust (kN)	Stress (MPa)
D0	30	29.5	2275	–	29.4	3812	–
D1	30	30	2518	0.57	30	2366	0.60
D2	30	29.7	2720	-0.04	29.7	2861	0.03
D3	30	29.7	2912	0.14	30	2760	0.16
D4	30	30	2639	0.25	29.8	2952	0.29
D5	30	30	2396	1.03	29.7	2912	1.11
D6	30	29.4	2194	–	29.6	3458	–

Warning risk levels for the strain of the concrete is shown in Table 2. When the lifting beam reaches 4.0 cm, the displacement, stress, and jack thrust results can be seen in Fig. 30 to Fig. 32. By analyzing the calculated limit state, the threshold of critical risk assessment is determined. Instead, other risk levels are determined by applying reduction factors of 0.9, 0.8, 0.7, and 0.6 to the maximum value obtained from the theoretical calculation. The inside displacement of the curve is about 40 mm when the jacking beam reaches 4.0 cm. The thrust is from 2224 kN to 2912 kN. The concrete stress is from –0.06 MPa to 1.13 MPa. The outside displacement of the curve is about 40 mm when the jacking beam reaches 4.0 cm. The thrust is from 2386 kN to 3751 kN. The concrete stress is from –0.02 MPa to 1.17 MPa.

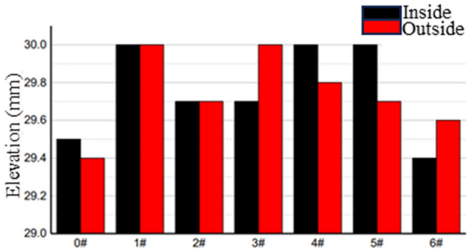

Fig. 27. Displacement diagram with a lifting height of 3.0 cm

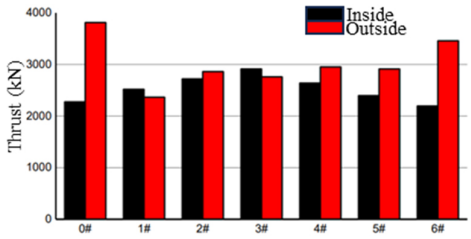

Fig. 28. Thrust diagram of a 3.0 cm lifting height jack

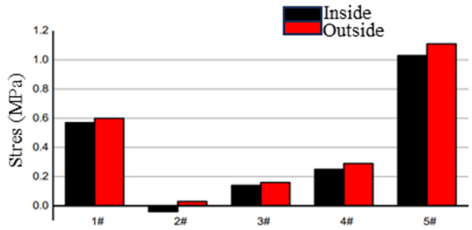

Fig. 29. Stress diagram with a lifting height of 3.0 cm

Table 2. Warning risk levels for the strain of the concrete (unit: MPa)

Location	Low Risk	Middle Risk	To Be Determine	High Risk	Critical
Color	Blue	Green	Yellow	Purple	Red
D0	0.948	1.11	1.26	1.42	1.58
D1	0.948	1.11	1.26	1.42	1.58
D2	0.948	1.11	1.26	1.42	1.58
D3	0.948	1.11	1.26	1.42	1.58
D4	0.948	1.11	1.26	1.42	1.58
D5	0.948	1.11	1.26	1.42	1.58
D6	0.948	1.11	1.26	1.42	1.58

When the lifting beam reaches 6.0 cm, the displacement, stress, and jack thrust results can be seen in Fig. 33 to Fig. 35. The inside displacement of the curve is about 60 mm when the jacking beam reaches 6.0 cm. The thrust is from 2275 kN to 2932 kN. The concrete stress is from –0.13 MPa to 0.38 MPa. The outside displacement of the curve is about 60 mm when the jacking beam reaches 6.0 cm. The thrust is from 2386 kN to 3852 kN. The concrete stress is from –0.07 MPa to 0.41 MPa.

When the beam drops to 2.0 cm, the displacement, stress, and jack thrust results can be seen in Fig. 36 to Fig. 38. The inside displacement of the curve is about 20 mm when the jacking beam reaches 2.0 cm. The thrust is from 2103 kN to 2831 kN. The concrete stress is

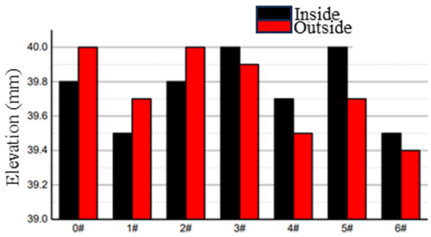

Fig. 30. Displacement diagram with a lifting height of 4.0 cm

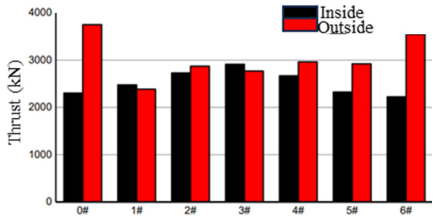

Fig. 31. Thrust diagram of a 4.0 cm lifting height jack

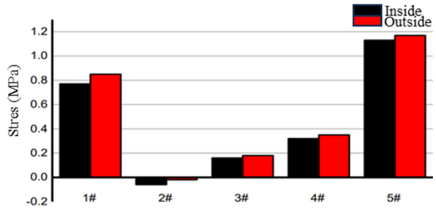

Fig. 32. Stress diagram with a lifting height of 4.0 cm

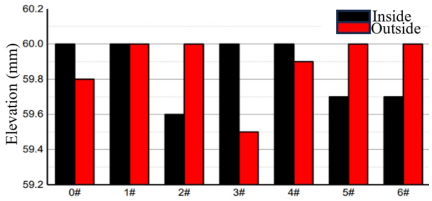

Fig. 33. Displacement diagram with a lifting height of 6.0 cm

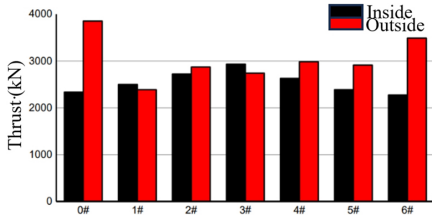

Fig. 34. Thrust diagram of a 6.0 cm lifting height jack

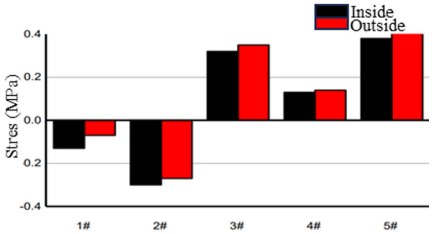

Fig. 35. Stress diagram with a lifting height of 6.0 cm

from –0.14 MPa to 0.62 MPa. The outside displacement of the curve is about 20 mm when the jacking beam reaches 2.0 cm. The thrust is from 2315 kN to 3630 kN. The concrete stress is from –0.09 MPa to 0.64 MPa.

When the beam drops to 6.0 cm, the displacement and hydraulic pressure results can be seen in Fig. 39 to Fig. 41. The inside displacement of the curve is about 60 mm when the jacking beam reaches 6.0 cm. The thrust is from 2083 kN to 2861 kN. The concrete stress is

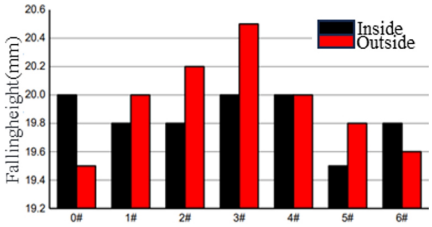

Fig. 36. Displacement graph of the drop height of 2.0 cm

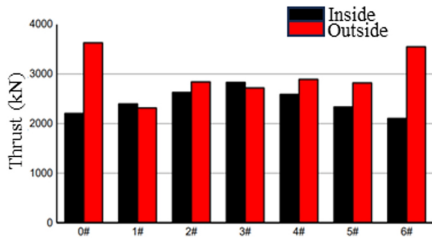

Fig. 37. Jack thrust graph of the drop height of 2.0 cm

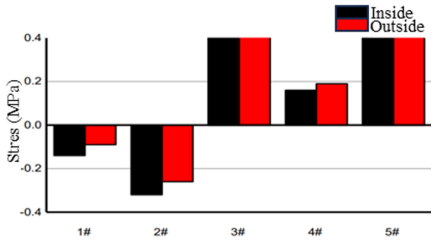

Fig. 38. Stress graph of the drop height of 2.0 cm

from –0.13 MPa to 1.08 MPa. The outside displacement of the curve is about 60 mm when the jacking beam reaches 6.0 cm. The thrust is from 2315 kN to 3620 kN. The concrete stress is from –0.07 MPa to1.13 MPa.

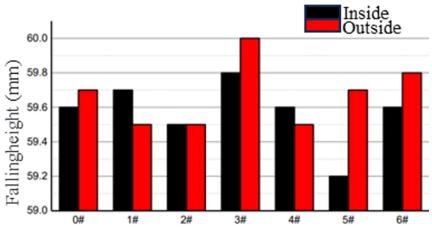

Fig. 39. Displacement graph of the drop height of 6.0 cm

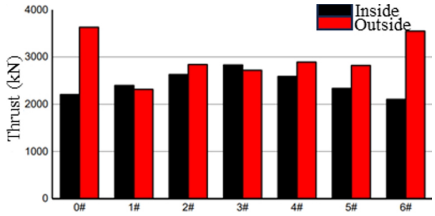

Fig. 40. Jack thrust graph of the drop height of 6.0 cm

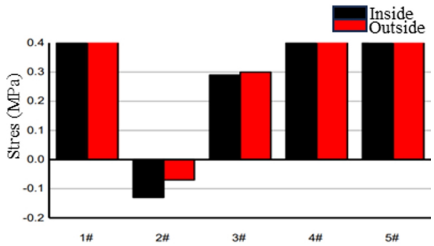

Fig. 41. Stress graph of the drop height of 6.0 cm

During the bridge lifting construction process, various values such as displacement, stress, and oil pressure are monitored. Based on the monitored data, it is known that the maximum stress in the structure during the lifting process did not reach the concrete's ultimate tensile stress, and the displacement and oil pressure were within the controlled range. As a result, no damage was caused to the beam structure, and the lifting construction process was considered safe and reliable.

6.2. Analysis of monitoring data during the translation process

The repositioning process is divided into three working conditions, and the number of lifting operations for each condition is shown in Table 3.

Table 3. The table of bridge repositioning working conditions

Pivot displacement	Top-up frequency		
	Operating condition 1 (mm)	Operating condition 2 (mm)	Operating condition 3 (mm)
D0	10	5	14
D1	10	5	14
D2	10	5	14
D3	–	–	–
D4	12	16	31
D5	12	16	31
D6	12	16	31

1. Beam repositioning displacement as shown in Fig. 42 and Fig. 43.

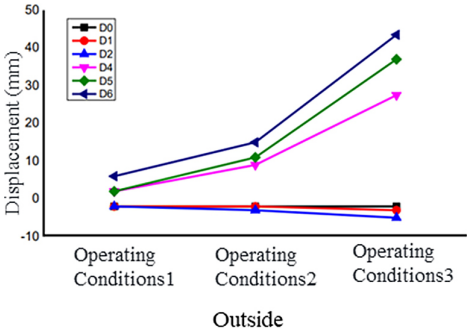

Fig. 42. Displacement diagram of repositioning on the inner side of the curve

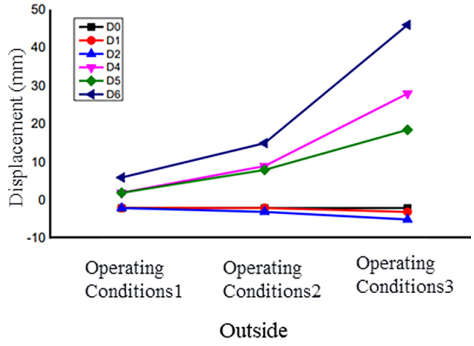

Fig. 43. Displacement diagram of repositioning on the outer side of the curve

2. Top pushing force results of beam translation repositioning as shown in Fig. 44 and Fig. 45.

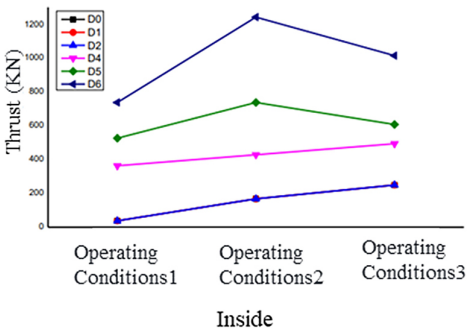

Fig. 44. Top pushing force diagram of repositioning on the inner side of the curve

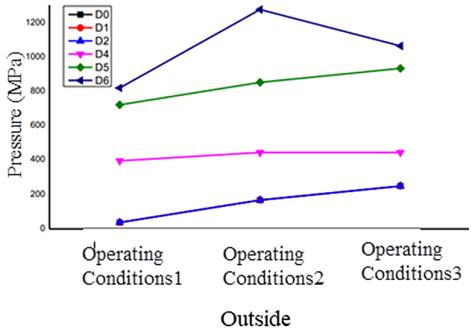

Fig. 45. Top pushing force diagram of repositioning on the outer side of the curve

3. Stress results of beam repositioning as shown in Fig. 46 and Fig. 47.

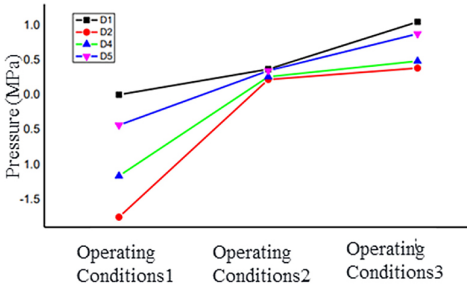

Fig. 46. Stress value diagram of repositioning on the inner side of the curve

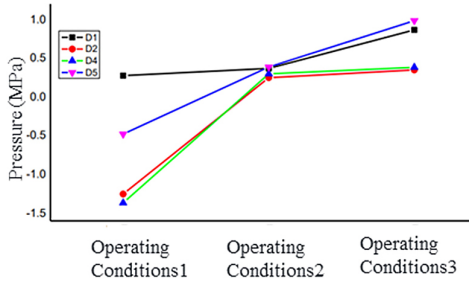

Fig. 47. Stress value diagram of repositioning on the outer side of the curve

During the bridge translation construction process, monitoring data such as displacement, stress, and oil pressure are used to determine that the structure mainly undergoes rigid body rotation during the jacking process. The maximum stress on the main beam is far below the concrete cracking limit stress value, and the displacement and oil pressure are also within the control range. No damage has been caused to the beam structure, and the jacking construction process is safe and reliable.

7. Conclusions

The main purpose of this study is to combine the use of engineering and real-time monitoring based on the monitoring plan to monitor the stress and displacement of the beam during the jacking and translation construction process. The reaction forces of each support

during the construction process are also monitored, and the jacking force is controlled to ensure the stability and safety of the beam during construction. Finally, the jacking and translation monitoring data are compared and analyzed with the theoretical calculated values. The following conclusions were obtained:

1. In the actual construction, the stress at the middle of the control sections at the bottom and the jacking height of the main beam, as well as the jacking force, were monitored during the jacking heights of 3.0 cm, 4.0 cm, 6.0 cm, and the beam dropping heights of 2.0 cm and 6.0 cm. The monitoring data indicated that the stress values generated during the jacking stage were below the stress control standards, and no voids occurred at the supports.
2. The translation construction employed a whole bridge jacking and resetting method, and the entire bridge was monitored during three different working conditions. The stress increments at sections 2# and 4# were relatively small, and the measured stress increments across the entire bridge were below the stress control standards. The displacements at the bridge abutments were also small and did not come into contact with the abutment blocks. No significant elastic deformation was observed, thus achieving the jacking and resetting of the bridge.

References

[1] J.F. Hajjar, D. Krzmarzick, and L. Pallarés, "Measured behavior of a curved composite I-girder bridge", *Journal of Constructional Steel Research*, vol. 66, no. 3, pp. 351–368, 2010, doi: 10.1016/j.jcsr.2009.10.001.

[2] A. Marcello, M.F. Granata, and M. Oliva, "Influence of secondary torsion on curved steel girder bridges with box and I-girder cross-sections", *KSCE Journal of Civil Engineering*, vol. 19, pp. 2157–2171, 2015, doi: 10.1007/s12205-015-1373-1.

[3] H. Gao, H. Duan, and Y. Sun, "Evaluation of bearing capacity of multi-span spandrel-braced stone arch bridge based on static load test", *Archives of Civil Engineering*, vol. 68, no. 4, pp. 633–651, 2022, doi: 10.24425/ace.2022.143059.

[4] W. Erqiang, et al., "Implication of bridge resilience design and lessons from negative examples", *Advances in Bridge Engineering*, vol. 3, no. 1, art. no. 23, 2022, doi: 10.1186/s43251-022-00077-8.

[5] M.F. Granata, "Analysis of non-uniform torsion in curved incrementally launched bridges", *Engineering Structures*, vol. 75, pp. 374–387, 2014, doi: 10.1016/j.engstruct.2014.05.047.

[6] J. Ju, X.F. Zhu, and H.F. Ren, "Deformation analysis of short and medium span curved beam bridge", *Applied Mechanics and Materials*, vol. 347-350, pp. 3546–3549, 2013, doi: 10.4028/www.scientific.net/AMM.347-350.3546.

[7] S.J. Fatemi, M.S. Mohamed Ali, and A.H. Sheikh, "Load distribution for composite steel–concrete horizontally curved box girder bridge", *Journal of Constructional Steel Research*, vol. 116, pp. 19–28, 2016, doi: 10.1016/j.jcsr.2015.08.042.

[8] Z. Shuang, et al., "Sectional model wind tunnel test and research on the wind-induced vibration response of a curved beam unilateral stayed bridge", *Buildings*, vol. 12, no. 10, art. no. 1643, 2022, doi: 10.3390/buildings12101643.

[9] H. Sungnam, "Effect of prestress levels and jacking methods on friction losses in curved prestressed tendons", *Applied Sciences*, vol. 7, no. 8, art. no. 824, 2017, doi: 10.3390/app7080824.

[10] Y. Xinbo, et al., "Analysis on the Stability of Top Pushing Construction of Curved Steel Box Beam of a Cross-sea Bridge", *IOP Conference Series: Earth and Environmental Science*, vol. 769, no. 2, 2021, doi: 10.1088/1755-1315/769/3/032027.

[11] L. Yung Bin, et al., "Online monitoring of highway bridge construction using fiber Bragg grating sensors", *Smart Materials and Structures*, vol. 14, no. 5, art. no. 1075, 2005, doi: 10.1088/0964-1726/14/5/046.

[12] F. Saman and A. Mehrabi, "Health monitoring of closure joints in accelerated bridge construction: A review of non-destructive testing application", *Journal of Advanced Concrete Technology*, vol. 17, no. 7, pp. 381–404, 2019, doi: 10.3151/jact.17.381.

[13] R.M. Choudhry, et al., "Cost and schedule risk analysis of bridge construction in Pakistan: Establishing risk guidelines", *Journal of Construction Engineering and Management*, vol. 140, no. 7, 2014, doi: 10.1061/(ASCE)CO.1943-7862.0000857.

[14] S. Yuzhong, et al., "The impact of transformational leadership on safety climate and individual safety behavior on construction sites", *International Journal of Environmental Research and Public Health*, vol. 14, no. 1, art. no. 45, 2017, doi: 10.3390/ijerph14010045.

[15] M. Kesavan, et al., "A curriculum guide model to the next normal in developing construction supervisory training programmes", *Built Environment Project and Asset Management*, vol. 12, no. 5, pp. 792–822, 2022, doi: 10.1108/BEPAM-02-2021-0038.

Received: 2023-10-17, Revised: 2023-12-28